

# Dynamics of Cosmic Strings in Schwarzschild Spacetime

Jean-Pierre De Villiers  
*Theoretical Physics Institute*  
*Department of Physics*  
*University of Alberta*  
*Edmonton, Canada T6G 2J1*

June 28, 2017

## **Abstract**

Cosmic strings are topological defects thought to have formed early in the life of the universe. If such objects exist, a study of their interaction with black holes is of interest. The equations of motion of a cosmic string have the form of highly non-linear wave equations. General analytic solutions, except for motion in certain backgrounds such as flat and shockwave spacetimes, remain unknown; consequently, much of the work must be carried out numerically. To do this, an implicit finite difference scheme was developed that involves solving large block tridiagonal systems. This paper discusses the numerical method, its validation against analytic and semi-analytic solutions, and preliminary results on the interaction of a cosmic string with Schwarzschild black holes.

# 1 Introduction

This paper <sup>1</sup> discusses numerical solutions to the equations of motion of a cosmic string in black hole spacetimes. Strings can be either closed (a loop) or open. Open strings can be of infinite length, or they can be terminated by monopoles; strings can also terminate on the horizon of a black hole (due to earlier capture). From the numerical point of view, cosmic strings of finite length are preferable since they lead directly to finite computational domains. The goal is to model the string as a segment terminated by massive end points, taking the limit where the masses go to infinity to simulate an infinite open string.

A cosmic string is an extended object under tension; motion of the string near a black hole represents the resultant of the competing influences of tension and gravity. The results presented here concern the deformations induced by the gravitational field of Schwarzschild black holes. These results will be compared to the behaviour of dust strings, one-dimensional distributions of test particles that mimic a string with no tension.

## 2 Equations of Motion of a Cosmic String

The equations of motion for a cosmic string with massive end points are derived from an action functional. Solutions to these equations describe the world surface of the string as functions  $x^\mu(\xi^0, \xi^1)$  of the string parameters  $\xi^A (A = 0, 1)$  conventionally shown as  $(\xi^0, \xi^1) \equiv (\tau, \sigma)$ . The derivation builds upon two sources, Larsen and Frolov [6], who obtain equations of motion for open strings in arbitrary backgrounds, and Barbashov [3], who obtains equations of motion for strings with massive end points in Minkowski spacetime. The action for a string terminated by massive end points in an arbitrary spacetime is taken to be,

$$\begin{aligned} S[x^\mu, h_{AB}, \sigma_i] &= -\mu \int_{\tau_1}^{\tau_2} d\tau \int_{\sigma_1(\tau)}^{\sigma_2(\tau)} d\sigma \sqrt{-h} h^{AB} G_{AB} \\ &\quad - \sum_{i=1}^2 \frac{m_i}{2} \int_{\lambda_1}^{\lambda_2} d\lambda g_{\mu\nu} \frac{dx^\mu}{d\lambda} \frac{dx^\nu}{d\lambda} \end{aligned} \quad (1)$$

---

<sup>1</sup>Preprint: Alberta Thy 12-97. To appear in Proceedings of Seventh Canadian Conference on General Relativity and Relativistic Astrophysics (Fall 1997)

where  $\mu$  is the string tension;  $\sigma_i(\tau)$  represent the motion of the end points in the 2D parameter space of the string;  $h_{AB}$  is the metric of the string parameter space, with determinant  $h$ ;  $G_{AB} \equiv g_{\mu\nu} \frac{\partial x^\mu}{\partial \xi^A} \frac{\partial x^\nu}{\partial \xi^B}$  is the induced metric on the string worldsheet; and  $\lambda \equiv \lambda(\tau)$  is the most general parametrization for the end points whose motion is described by  $x^\mu(\lambda(\tau), \sigma_i(\tau))$ .

The end points are taken to represent the mass of a longer (potentially infinite) string lying outside the region of interest; the motion of these points represents a boundary condition for the section of the string worldsheet under study. In the limit of infinite mass, these end points move along geodesics.

The equations of motion are obtained by taking the  $h_{AB}$ ,  $x^\mu$ , and  $\sigma_i$  variations of the action. The details of this derivation are given elsewhere [4]. The internal string coordinates are chosen such that  $\tau$  is a time-like coordinate, and  $\sigma$  a spatial coordinate used to parametrize points along the string. The resulting equations of motion for the interior of the string and boundary conditions are,

$$\frac{\partial^2 x^\mu}{\partial \tau^2} + \Gamma^{\mu}_{\rho\eta} \frac{\partial x^\rho}{\partial \tau} \frac{\partial x^\eta}{\partial \tau} = \begin{cases} \frac{\partial^2 x^\mu}{\partial \sigma^2} + \Gamma^{\mu}_{\rho\eta} \frac{\partial x^\rho}{\partial \sigma} \frac{\partial x^\eta}{\partial \sigma}; & (-\frac{\pi}{2} < \sigma < \frac{\pi}{2}) \\ 0; & (\sigma = \pm \frac{\pi}{2}) \end{cases} \quad (2)$$

along with constraints,

$$\begin{aligned} g_{\mu\nu} \left[ \frac{\partial x^\mu}{\partial \tau} \frac{\partial x^\nu}{\partial \tau} + \frac{\partial x^\mu}{\partial \sigma} \frac{\partial x^\nu}{\partial \sigma} \right] &= 0; & (-\frac{\pi}{2} < \sigma < \frac{\pi}{2}) \\ g_{\mu\nu} \left[ \frac{\partial x^\mu}{\partial \tau} \frac{\partial x^\nu}{\partial \sigma} \right] &= 0; & (-\frac{\pi}{2} < \sigma < \frac{\pi}{2}) \\ \frac{d}{d\tau} \left( g_{\mu\nu} \left[ \frac{dx^\mu}{d\tau} \frac{dx^\nu}{d\tau} \right] \right) &= 0; & (\sigma = \pm \frac{\pi}{2}) \end{aligned} \quad (3)$$

which are used as checks on the quality of the numerical solutions to (2).

### 3 Discretization of the Equations of Motion

The above equations have the form of non-linear wave equations. Ames [2] describes a discretization due to Von Neumann for the linear wave equation,  $u_{\tau\tau} = u_{\sigma\sigma}$ , which uses a standard second-order centered difference formula

for evaluating the time derivative at the discrete grid point  $u(\sigma_i, \tau_j)$ , and a weighted average (weighting parameter  $\lambda$ ) of centered spatial differences at three adjacent time steps,  $\tau_{j-1}$ ,  $\tau_j$ , and  $\tau_{j+1}$ . This averaging gives rise to a 9-point implicit scheme. Von Neumann's discretization must be extended to handle a system of equations and the non-linear terms containing Christoffel symbols. To simplify the notation, denote  $x^\mu(\sigma_i, \tau_j) \equiv \mathbf{x}_{i,j}$ . The second-order time derivative is discretized using a centered difference formula on a non-uniform mesh (to accommodate the iterative scheme described below),

$$\left(\frac{\partial^2 \mathbf{x}}{\partial \tau^2}\right)_{i,j} \approx \frac{2}{\Delta\tau_j + \Delta\tau_{j+1}} \left\{ \frac{1}{\Delta\tau_{j+1}} (\mathbf{x}_{i,j+1} - \mathbf{x}_{i,j}) - \frac{1}{\Delta\tau_j} (\mathbf{x}_{i,j} - \mathbf{x}_{i,j-1}) \right\} \quad (4)$$

while the second-order spatial derivative is discretized using the standard centered difference, denoted  $D^2\mathbf{x}_{i,j}$ , as an average of three time levels,

$$\left(\frac{\partial^2 \mathbf{x}}{\partial \sigma^2}\right)_{i,j} \approx \frac{\lambda}{(\Delta\sigma)^2} D^2\mathbf{x}_{i,j+1} + \frac{(1-2\lambda)}{(\Delta\sigma)^2} D^2\mathbf{x}_{i,j} + \frac{\lambda}{(\Delta\sigma)^2} D^2\mathbf{x}_{i,j-1} \quad (5)$$

The non-linear spatial term, denoted  $H$  for compactness, is also discretized using the averaging method,  $(H)_{i,j}^n \approx \lambda H_{i,j+1}^n + (1-2\lambda) H_{i,j}^n + \lambda H_{i,j-1}^n$ , where the upper index is an iteration index. The contributions at the  $j$  and  $j-1$  level can be obtained directly from centered differences, evaluating the Christoffel symbols (using analytic expressions) at  $\mathbf{x}_{i,j}$  and  $\mathbf{x}_{i,j-1}$ . The  $j+1$  term is linearized through a Taylor expansion,  $H_{i,j+1}^{n+1} \cong H_{i,j+1}^n + J(\mathbf{x}_{i,j+1}^n) \bullet \Delta\mathbf{x}_{i,j+1}^n$  where  $\Delta\mathbf{x}_{i,j+1}^n$  represents the difference between the iterated solutions at the  $j+1$  time-level,  $\Delta\mathbf{x}_{i,j+1}^n = \mathbf{x}_{i,j+1}^{n+1} - \mathbf{x}_{i,j+1}^n$ , and  $J(\mathbf{x})$  is the Jacobian of the  $n$ -th iteration of  $H_{i,j+1}^n$ . The temporal non-linear term is expanded using centered differences on a non-uniform temporal mesh and rearranged using the  $\Delta$ -notation introduced above. This term is linearized directly by discarding terms of order  $\Delta\mathbf{x}^2$ .

The various difference expressions are combined and the terms involving the iterated solution,  $\Delta\mathbf{x}_{i,j+1}^n$ , isolated on the right hand side. The system reduces to an equation for the components of a block-tridiagonal system,

$$A_{i-1,j+1}^n \bullet \Delta\mathbf{x}_{i-1,j+1}^n + B_{i,j+1}^n \bullet \Delta\mathbf{x}_{i,j+1}^n + C_{i+1,j+1}^n \bullet \Delta\mathbf{x}_{i+1,j+1}^n = d_{i,j+1}^n \quad (6)$$

where  $A$ ,  $B$ , and  $C$  are  $4 \times 4$  matrices and  $d$  is a 4-vector. The block-tridiagonal system expresses an implicit relationship between the iterated

solution at all points on the spatial grid (of  $N$  points) and reduces to the matrix expression  $T^n \bullet \Delta \vec{x}^n = \vec{d}^n$  where  $T$  in an  $N \times N$  matrix whose elements are  $4 \times 4$  matrices, and  $\vec{x}^n$  and  $\vec{d}^n$  are vectors of length  $N$  whose elements are 4-vectors. The iterated solution for the new time level is found by inverting matrix  $T$ ; the process is repeated until the solution converges (i.e. produces a zero  $d$ -vector). Failure to converge triggers a time-step reduction mechanism; if this mechanism fails to find a suitable new step size, the solution is stopped. The constraint equations (3) are invoked periodically to assess the quality of the solution by computing an average value (and standard deviation) for the constraints over the spatial grid.

## 4 Testing and Using the Solver

The finite difference expressions were coded and tested against an analytic flat space solution (in spherical-polar coordinates so as to test the non-linear portions of the code) and a semi-analytic shockwave solution. The former test established the accuracy of the method, the latter tested the iterative scheme at the ultra-relativistic extreme.

### 4.1 Minkowski Spacetime

An analytic expression is easily obtained for a cosmic string of length  $L$  moving at constant velocity  $v$  in Minkowski spacetime. In Cartesian coordinates, the string is oriented along the  $z$ -axis, such that  $Z(\tau, \sigma) = L\sigma/\pi$ ,  $(-\frac{\pi}{2} \leq \sigma \leq \frac{\pi}{2})$ , with motion taking place along the  $x$ -axis. The motion is described by,

$$\mathbf{x}(\tau, \sigma) = \left( \frac{L}{\pi} \cosh(\beta) \tau + T_0, \frac{L}{\pi} \sinh(\beta) \tau + X_0, Y_0, \frac{L}{\pi} \sigma \right) \quad (7)$$

where  $X_0$ ,  $Y_0$ , and  $T_0$  represent arbitrary initial values. The parameter  $\beta$  represents the rapidity of a string moving with velocity  $v = \tanh \beta$ . This solution was coded in spherical-polar coordinates to exercise the non-linear portions of the code, and is compared to the numeric solution in Figure 1, where the absolute relative error averaged over the spatial grid is plotted as a function of string proper time,  $\tau$ . The graph covers roughly 10,000 time

steps, and the slope confirms that the method is second-order in the time step size  $\Delta\tau$ .

This solution (expressed in Schwarzschild coordinates,  $(t, r, \theta, \phi)$ ) is also used as initial data for all numerical work, since black hole spacetimes of interest are asymptotically flat. The initial time  $t_0$  is taken to be zero. The value of  $r_0$  sets the initial distance from the black hole and is chosen to make the error of the analytic solution small. The value of  $\phi_0$  sets the initial impact parameter  $b$  ( $b = r_0 \sin \phi_0$ ) relative to the black hole. The string is oriented symmetrically about the equatorial plane.

## 4.2 Shockwave Spacetime

The shockwave spacetime arises when an extremely relativistic string passes near a black hole. In this situation, the string effectively propagates in Minkowski spacetime up to the point where it encounters the sharply defined gravitational potential of the black hole.

In the limit where string velocity  $v \rightarrow c$ , the Schwarzschild and Kerr metrics can be reduced to a shockwave form (Hayashi and Samura, [5]),

$$ds^2 = -du dv + dy^2 + dz^2 - 4p g(\rho) \delta(u) du^2 \quad (8)$$

where,

$$u = t - x; v = t + x; p = \gamma M_{BH}; \rho = \sqrt{y^2 + z^2} \quad (9)$$

and, for the Schwarzschild case,

$$g(\rho) = \ln \rho^2 - \frac{\rho}{4 M_{BH}} \left[ \pi - 4 \sqrt{1 - \frac{4 M_{BH}^2}{\rho^2}} \arctan \sqrt{\frac{\rho + 2 M_{BH}}{\rho - 2 M_{BH}}} \right] \quad (10)$$

In this metric, the string is propagating in the x-direction and the coordinates y and z are transverse to the motion. Spacetime is everywhere flat, except at  $u = 0$ , so the flat-space constant velocity solutions are used as a starting point. The equations of motion of strings in a shockwave background can be expressed as a Fourier series (adapted from Amati and Klimcik, [1]),

$$\begin{aligned} U(\sigma, \tau) &= p^u \tau \\ V(\sigma, \tau) &= v_0 + p^v \tau + i \sum_{n \neq 0} \frac{\alpha_n^v}{n} e^{-in\tau} \cos(n\sigma) \end{aligned}$$

$$\begin{aligned}
Y(\sigma, \tau) &= b + p^y \tau + i \sum_{n \neq 0} \frac{\alpha_n^y}{n} e^{-in\tau} \cos(n\sigma) \\
Z(\sigma, \tau) &= \frac{L}{\pi} \left( \sigma - \frac{\pi}{2} \right) + p^z \tau + i \sum_{n \neq 0} \frac{\alpha_n^z}{n} e^{-in\tau} \cos(n\sigma) \quad (11)
\end{aligned}$$

where  $p^\alpha$  is the  $\alpha$ -component of the string's 4-momentum, and the Fourier coefficients for the  $Y$  and  $Z$  solutions are given by,

$$\alpha_n^i = \frac{p^u}{2\pi} \int_0^\pi \partial_i f(X(\sigma, 0)) \cos(n\sigma) d\sigma \quad (12)$$

where  $f(X(\sigma, 0)) = -4p g(X(\sigma, 0))$ , and  $\alpha_n^i$  is evaluated numerically.

It is possible to compare this series expansion with numerically-generated solutions for a string moving at ultra-relativistic velocity. The most interesting comparison is made for projections of the worldsheet onto the Y-Z plane. Figure 2 shows the numerically generated solution, the shockwave series solution (to 300 terms), and a numerically generated dust string solution where an array of test particles with identical initial data as the cosmic string are propagated using the geodesic equation for test particles.

### 4.3 Close Encounters

A cosmic string straying too close to a black hole will become trapped; the conditions under which this happens, expressed in terms of the 2D parameter space of initial velocity  $v$  and impact parameter  $b$ , can be used to generate a plot of the critical impact parameter (a line in b-v space). These results are discussed in a separate paper [4]. The previous section discussed the excitation of ultra-relativistic strings; here we consider the case of a string moving more slowly. The study of geodesics of particles shows that for impact parameters near the critical value, particles can execute a partial orbit around the black hole before escaping. Figure 3 shows the trajectory of a slow string with near-critical impact parameter, displaying a time-sequence for the portion of a string in the immediate vicinity of the equatorial plane, which shows the string attempting a partial orbit before being pulled back into its original direction of motion.

## 5 Discussion

In this paper, equations of motion for a cosmic string were derived from an action that deals with a finite string terminated by massive end points. The end points are taken to represent the mass of segments (potentially infinite) lying outside the region of interest; the motion of these points represents a boundary condition for the section of the string worldsheet under study. In the limit of infinite mass, these end points move along geodesics. The equations of motion for the interior of the worldsheet have the form of highly non-linear wave equations.

A numerical method was developed based on Von Neumann's discretization of the wave equation. The discretized equations are linearized and give rise to a block-tridiagonal system of equations that must be solved iteratively to advance the solution in time.

The validation of this method against analytic solutions in Minkowski spacetime and semi-analytic solutions in shockwave spacetimes was discussed, as well as a comparison against dust strings. The excitation of a slowly moving string with impact parameter near the critical parameter for trapping was also shown.

These results illustrate the role of tension in determining the dynamics of the string. At ultra-relativistic speeds, a string develops a strong excitation in the direction normal to its original motion. The cosmic string and the dust string both exhibit loop formation immediately following the encounter, as portions of the strings nearest the equatorial plane cross over to the other side. Whereas the portions of the dust string undergoing this cross-over continue in their new direction, those portions of the cosmic string that have undergone a cross-over eventually recross the equatorial plane, giving the worldsheet a kink-like profile that propagates outward along the string. At lower velocities, with near-critical impact parameters, loop formation is also observed, this time in the direction of motion. The cosmic string performs a partial orbit, but eventually gets pulled back in the original direction of motion, giving rise to the looping structure. The time sequence shown in Figure 3 is for a string with initial impact parameter of  $2.28 r_g$ ; this value is less than the minimum impact parameter of  $\sim 2.6 r_g$  for particles (which occurs at the ultra-relativistic limit). Numerical studies of the trapping of cosmic strings has shown that they are much more difficult to trap than particles; this will be discussed in greater detail in [4].



## References

- [1] Amati, D., and Klimcik, C. Strings in a shockwave background and generation of curved geometry from flat-space string theory. Phys. Lett. **B210** 92-96 (1988).
- [2] Ames, W.F. Non-linear Partial Differential Equations in Engineering. Academic Press. 1965
- [3] Barbashov, B.M., Some solutions of the equations of motion of a relativistic string with massive ends. Nucl. Phys., **B129**, 175-188 (1977).
- [4] De Villiers, J.P., and Frolov, V.P., Numerical Study of the Motion of Cosmic Strings in Black Hole Spacetimes. *in preparation*.
- [5] Hayashi, K., and Samura, T. Gravitational shock waves for Schwarzschild and Kerr black holes. Phys. Rev. **D50** 3666-3676 (1994).
- [6] Larsen, A.L., and Frolov, V.P., Propagation of perturbations along strings, Nucl. Phys., **B414**, 129-146 (1994).

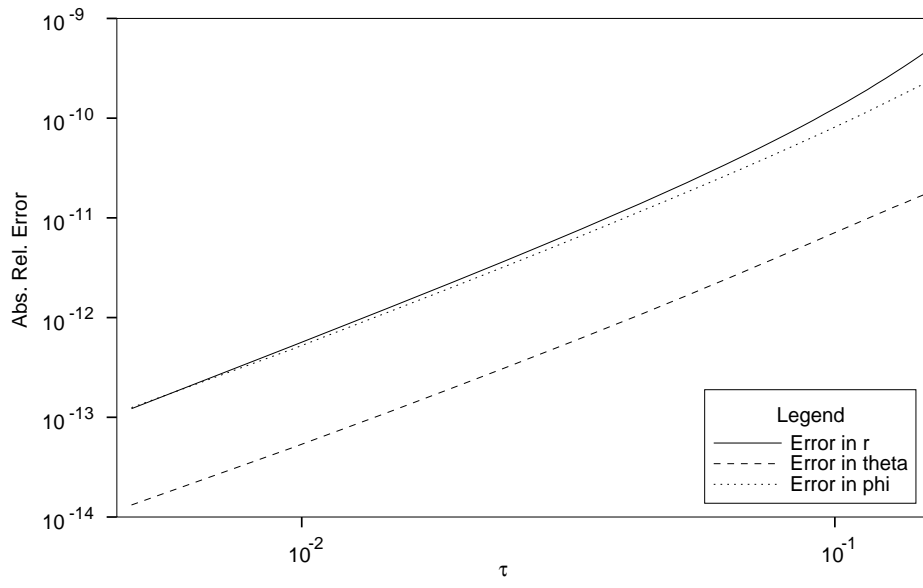


Figure 1: Comparison of numerical solution to analytic solution in Minkowski spacetime.

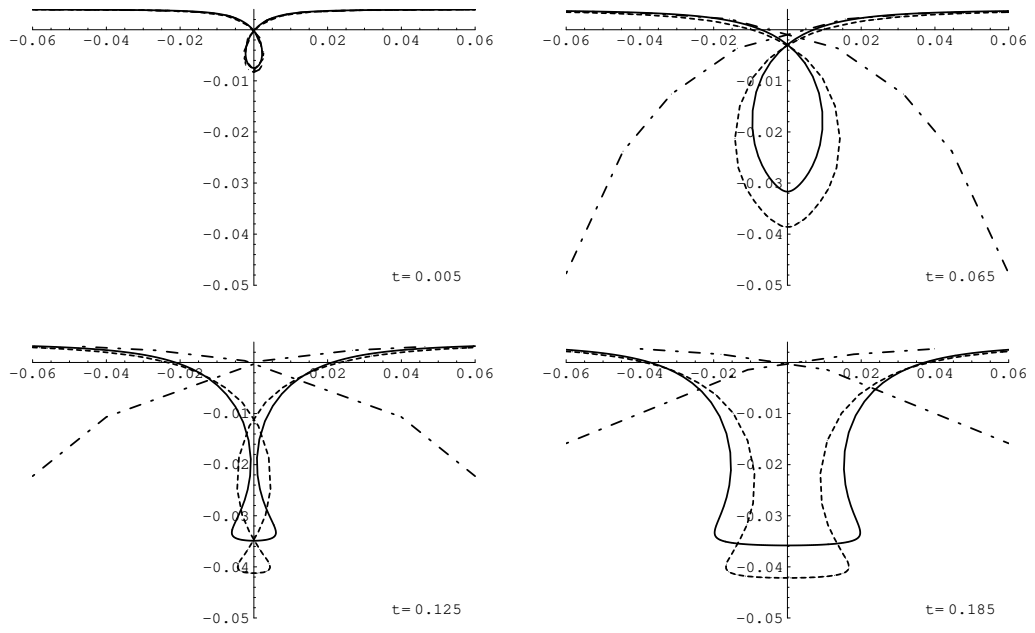


Figure 2: Comparison of numerical solution (solid line) to shockwave (dashed) and dust (dash-dot) solutions. Initial velocity,  $0.995c$ , impact parameter  $4 r_g$ .

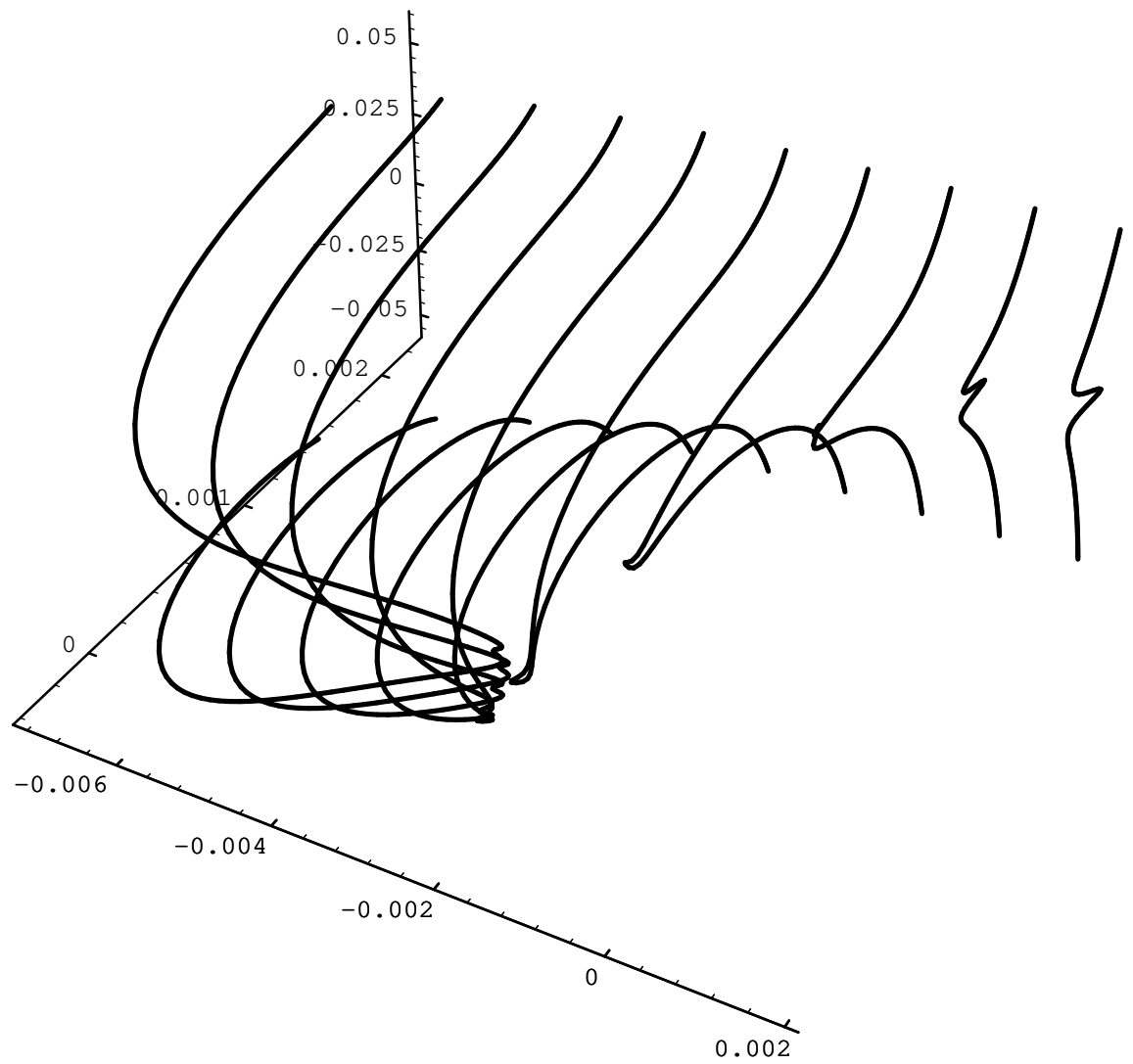


Figure 3: Time sequence of string close encounter. Black hole lies at origin of coordinate system. Initial velocity,  $0.125c$ , impact parameter  $2.28 r_g$ .